A study of nonrigid aromatic molecules by supersonic molecular jet spectroscopy. I. Toluene and the xylenes

P. J. Breen, J. A. Warren, and E. R. BernsteinJeffrey I. Seeman

A study of nonrigid aromatic molecules by supersonic molecular jet spectroscopy. I. Toluene and the xylenes

P. J. Breen, J. A. Warren, and E. R. Bernstein
Department of Chemistry, Condensed Matter Sciences Laboratory, Colorado State University, Fort Collins, Colorado 80523

Jeffrey I. Seeman
Philip Morris U.S.A. Research Center, Richmond, Virginia 23261

Dispersed emission and time of flight mass spectra are presented for jet-cooled toluene, and o-, m-, and p-xylene. The spectra exhibit features, typically within 100 cm^{-1} of the $S_1 \rightleftharpoons S_0$ origins, which are assigned to transitions associated with the internal rotation of the ring methyl groups. A model is developed which treats this methyl motion as that of a one-dimensional rigid rotor. The spacings of the peaks in the spectra are used to solve for the rotational constant B of the methyl rotor, and for the size and shape of the n-fold barrier to rotation (i.e., V_3, V_6, etc.) within this model. For toluene and p-xylene, the barrier is found to be small in both the ground (S_0) $(V_6 \sim 10 \text{ cm}^{-1})$ and excited (S_1) $(V_6 \sim 25 \text{ cm}^{-1})$ electronic states. For m-xylene, the ground state is again found to have a low barrier $(V_6 \sim 25 \text{ cm}^{-1})$, but the excited state has a potential barrier of $V_3 = 81$ cm^{-1}, $V_6 = -30$ cm^{-1}. The barrier to rotation of the ring methyl groups is observed to be the highest for o-xylene. In this case the ground state is found to have a rather large barrier $V_3 = 425$ cm^{-1}, $V_6 = 18$ cm^{-1} which changes to $V_3 \sim 166$ cm^{-1}, $V_3' \sim -25$ cm^{-1}, and $V_6 \sim 0$ cm^{-1} in the excited state. The V_3' term represents a potential cross term between the two methyl rotors. The use of a kinetic energy cross term with a weighting coefficient of 0.72 in the Hamiltonian is also required for an accurate description of the excited state of this isomer. Empirical force field (EFF) calculations are performed for toluene and the three xylenes using a molecular orbital–molecular mechanics (MOMM) algorithm. The EFF-MOMM calculations are in essential agreement with the spectroscopic results and the one-dimensional rigid rotor model.

I. INTRODUCTION

An increased knowledge of the torsional vibrations of molecules which are "nonrigid"—that is, capable of passing from one conformation to another—is desirable for several reasons. Little is known, for example, about the form or the magnitude of substituent–substituent and substituent–aromatic ring interactions in multiply substituted aromatic systems. Such information is necessary in order to predict the structures and dynamics of stable conformers.[1] Knowledge of the internal rotations of electronically excited nonrigid molecules is sparse despite their increased importance with respect to the chemistries of excited state molecules. In general, a clearer understanding of the potential energy surfaces of nonrigid molecules will lead to an improved understanding of their chemistry.[2,3]

Laser supersonic molecular jet spectroscopy offers a suitable means for studying internal rotations in nonrigid molecules since it combines the advantages of low sample temperature, minimized medium effects, and high spectral resolution. For example, recent laser molecular jet studies by Lubman et al.[4] on the o-, m-, and p-dihydroxybenzenes and by Ito et al.[5] on meta-substituted phenols and β-napthol demonstrate that the technique can resolve *cis* and *trans* isomers of substituted hydroxylated aromatics. In these investigations, features corresponding to the $S_1 \leftarrow S_0$ origin bands of such isomers are separated by tens to hundreds of wave numbers.

In another study by Ito et al.,[6] laser molecular jet spectroscopy was used to observe and characterize transitions within the $S_1 \leftarrow S_0$ origin band associated with the internal rotational levels of the methyl group in o-, m-, and p-fluorotoluene. They were able to establish differences in the potential barrier to rotation of the methyl group between the ground and excited states of all three molecules; in the case of o-fluorotoluene, a large change in the equilibrium orientation of the methyl group in the excited state relative to the ground state was determined.

We have used laser molecular jet spectroscopy to study the internal rotational levels of the methyl rotors in toluene and o-, m-, and p-xylene and present our findings here. The principal goal of this study is the demonstration that the techniques employed provide reliable information which agrees well with other studies performed on these molecules. In the succeeding paper,[7] we apply these techniques to a study of the n-propyltoluenes. Collectively, these molecules form an important basis for initiating new studies on more complex nonrigid species such as substituted aromatic heterocycles for which chromophore-substituent interactions are anticipated to be more involved and more important.

II. EXPERIMENTAL PROCEDURES

The time-of-flight mass spectrometer (TOFMS) chamber has been described previously.[8] TOFMS experiments utilize an R. M. Jordan pulsed valve. Helium is used

as the carrier gas except where specified, with backing pressures of 50–100 psig. All experiments are performed at room temperature.

Dispersed emission (DE) experiments are carried out in a fluorescence excitation (FE) chamber described previously.[8] $f/4$ optics are used to collect and focus the emission onto the slits of an $f/8$ 2051 GCA McPherson 1 m scanning monochromator with a dispersion of 2.78 Å/mm in third order of a 1200 groove/mm 1.0 μm blazed grating. Expansion of the gas into the chamber is achieved with a Quanta Ray PSV-2 pulsed valve with a 500 μ pinhole located ∼1 cm from the laser beam. Samples are placed inside the head of the valve and heated to 70 °C to achieve a greater concentration in the jet. Helium is used as the carrier gas at a pressure of ∼50 psig.

III. CALCULATIONS

The energy levels and wave functions for the motion of a one-dimensional hindered rigid rotor can be obtained by solving for the eigenvalues and eigenvectors of the Schrödinger equation:

$$\left[-B\frac{\partial^2}{\partial\phi^2} + V(\phi) \right]\Psi_s(\phi) = E_m\Psi_s(\phi) \tag{1}$$

in which

$$V(\phi) = 1/2 \sum_n V_n(1 - \cos n\phi) , \tag{2}$$

B is the rotational constant ($\hbar^2/2I$), I is the moment of inertia of the rotor, and ϕ is the torsion angle. The hindering potential term (2) is simply a Fourier cosine expansion of the general potential: in the case of methyl rotors, the terms in the expansion must be multiples of three, that is $n = 3, 6, 9, \ldots$. The potential form for toluene can be written as

$$V(\phi) = \tfrac{1}{2}V_6(1 - \cos 6\phi) . \tag{3}$$

The solution to Eq. (1) for an unhindered rigid rotor [$V(\phi) = 0$] is of the form

$$\psi_m(\phi) = \frac{1}{\sqrt{2\pi}}e^{\pm im\phi} \tag{4}$$

and

$$E_m = m^2 B . \tag{5}$$

Expansion of the hindered [$V(\phi) \neq 0$] rotor eigenfunctions of Eq. (1) by 21 free rotor eigenfunctions [Eq. (4)] ($m = 0, \pm 1, \ldots, \pm 10$) provides a suitable basis set within which to diagonalize the Hamiltonian matrix appropriate to Eq. (1). Parameters V_6 and B are adjusted to fit the experimental data for toluene.

A molecule with two methyl rotors (e.g., xylene) is slightly more complex and the Hamiltonian for the double rigid rotor takes the form

$$\mathscr{H}(\phi,\tau) = \left[-B\left(\frac{\partial^2}{\partial\phi^2} + \chi\frac{\partial}{\partial\phi}\frac{\partial}{\partial\tau} + \frac{\partial^2}{\partial\tau^2}\right) + V(\phi,\tau) \right], \tag{6}$$

in which χ is a parameter for the magnitude of the cross kinetic energy term. The potential energy term $V(\phi,\tau)$ is composed of individual rotor terms in addition to cross or interference terms depending on the difference between the

two angles. Again the Fourier cosine expansion of the potential is appropriate. One can then write

$$V(\phi,\tau) = \sum_n 1/2\{V_n(2 - \cos n\tau - \cos n\phi)$$
$$+ V'_n[\cos(n\tau - n\phi) - 2]\} . \tag{7}$$

Specifically, the cross potential term has the expanded form

$$\tfrac{1}{2}V'_n(\cos n\tau \cos n\phi + \sin n\tau \sin n\phi - 2) . \tag{8}$$

This development follows closely the results of Ref. 9(a). A more complete discussion of these cross potential terms can be found in Ref. 9(b).

The free double rotor [$V(\phi,\tau) = \chi = 0$] wave function appropriate for $\mathscr{H}(\phi,\tau)$ [Eq. (6)] is

$$\psi_{n,m}(\phi,\tau) = \frac{1}{2\pi}e^{\pm in\phi}e^{\pm im\tau} . \tag{9}$$

The eigenvalues and eigenvectors of the hindered double rigid rotor Hamiltonian Eq. (6) are solved for within a basis set of 625 of these functions, $\psi_{n,m}$.

The xylene isomers are treated within this model employing parameters B, χ, V_3, V_6, V'_3, and V'_6: the experimental xylene isomer spectra are fit by variation of these parameter values.

The energy levels for internal rotation of the methyl rotor are labeled according to the m quantum number of a one-dimensional rotor. The symmetry of the Hamiltonian is given by the appropriate molecular symmetry group,[10,11] which in the case of toluene, for example, is G_{12}. The integral

$$\langle \psi_{\text{elec}}\psi_{\text{con}} | M_e | \psi_{\text{con'}}\psi_{\text{elec'}} \rangle$$

is nonzero for the following methyl rotor transitions within the 0_0^0 band of the $^1A''_1 \leftarrow {}^1A'_1$ electronic transition:

$$A'_1 \leftrightarrow A'_1, \qquad A'_2 \leftrightarrow A'_2, \qquad E' \leftrightarrow E',$$
$$A''_1 \leftrightarrow A''_1, \qquad A''_2 \leftrightarrow A''_2, \qquad E'' \leftrightarrow E'',$$
$$A'_1 \leftrightarrow A''_1, \qquad A'_2 \leftrightarrow A''_2, \qquad E' \leftrightarrow E'',$$
$$A'_1 \leftrightarrow A'_2, \qquad A''_1 \leftrightarrow A''_2.$$

Transitions between levels of A and E symmetries are forbidden, as are the transitions $A'_1 \leftrightarrow A''_2$ and $A'_2 \leftrightarrow A''_1$.

The dependence of the energy of each internal rotational level on the model Hamiltonian parameters V_3 and V_6 is illustrated in Fig. 1 for a single methyl rotor, and in Fig. 2 for a molecule containing two noninteracting methyl rotors. Figure 1 illustrates that a change in the V_3 potential shifts the levels more rapidly than does a change in V_6. A free rotor will have a transition between the $1e''$ and $2e'$ levels at ∼15 cm^{-1}, and a transition between the $0a'_1$ and $3a''_1$ levels at ∼45 cm^{-1}. If the TOFMS shows peaks near 15 and 50 cm^{-1}, the methyl rotor is probably close to being a free rotor, since $V_3 \approx V_6 \approx 0$ (free rotor) is the only region of parameter space for which a match to the spectral features occurs at 15 and 50 cm^{-1}. This is also true for the double rotor case (Fig. 2).

If the barrier to rotation of the methyl rotor is unchanged in an $S_0 \leftrightarrow S_1$ transition, the $0a'_1 \to 0a'_1$ and $1e'' \to 1e''$ transitions will be coincident in energy and only one peak, representing both transitions, will be found at the origin. If the barrier to rotation changes, however, the $0a'_1 \to 0a'_1$ and
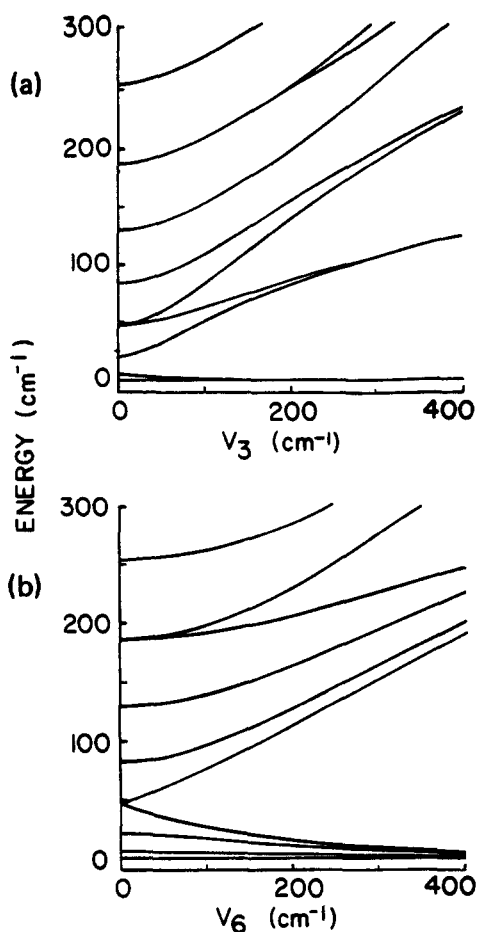
FIG. 1. Energies of the internal rotational levels of the methyl rotor in toluene with $B = 5.2$ cm^{-1} as a function of (a) a V_3 potential barrier, and (b) a V_6 potential barrier. For both cases, the symmetry labels for the rotational levels are, in order of increasing energy, at 5 cm^{-1} of potential barrier, $0a_1'$, $1e''$, $2e'$, $3a_2''$, $3a_1''$, $4e'$, $5e''$, $6a_2'$, $6a_1'$, $7e''$.

FIG. 2. Energies of the internal rotational levels of p-xylene (double rotor case) with $B = 5.2$ cm^{-1} as a function of (a) a V_3 potential barrier, and (b) a V_6 potential barrier. For both cases, the symmetry labels for the rotational levels are, in order of increasing energy at 5 cm^{-1} of potential barrier, $0a_1'0a_1'$, $0a_1'1e''$, $1e''1e''$, $0a_1'2e'$, $1e''2e'$, $2e'2e'$, $0a_1'3a_2''$, $0a_1'3a_1''$, $1e''3a_2''$, $1e''3a_1''$, $2e'3a_2''$, $2e'3a_1''$, $0a_1'4e'$, $1e''4e'$, $3a_2''3a_2''$, $3a_2''3a_1''$, and $3a_1''3a_1''$.

$1e'' \rightarrow 1e''$ transitions will occur at slightly different energies (depending on the magnitude of the change) and the origin of the spectrum will appear as a doublet. For a double rotor system with different barriers in the S_0 and S_1 states, the origin will appear as a triplet. Thus the nature of the potential well for internal rotation of the methyl group may often be ascertained from an initial examination of the spectrum.

Empirical force field (EFF) calculations are performed for toluene and the three xylenes using the molecular orbital–molecular mechanics (MOMM-85) algorithm of Kao et al.[12] This force field has been specifically parametrized for aromatic ring systems and is known to reproduce experimental geometries and energies. MOMM has also been used to correlate steric energies with the rates of certain aromatic ring reactions.[13] These ground state calculations are performed using complete geometry optimization to estimate the potential energy barriers to rotation about the $C_{aromatic}$ – C_α and C_α–C_β bonds, i.e., about the torsions (C_{ortho}–C_{ipso}–C_α–C_β) and (C_{ipso}–C_α–C_β–C_γ), respectively.

IV. RESULTS AND DISCUSSION

A. Toluene

Figure 3 shows the TOFMS of jet-cooled toluene for the 0_0^0 region of the first excited singlet state S_1. The origin is
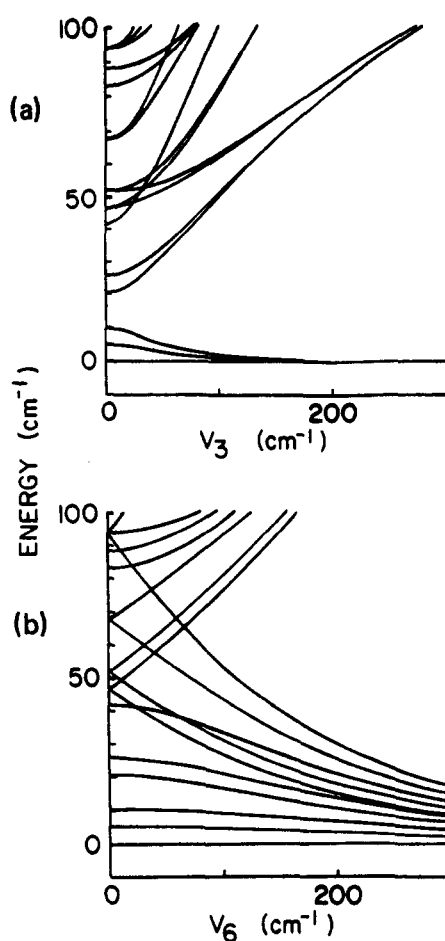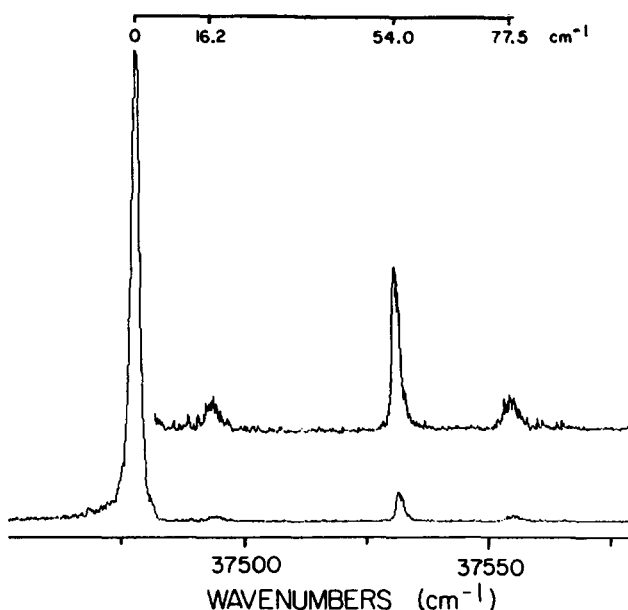

FIG. 3. One-color TOFMS of the 0_0^0 region of toluene. The origin occurs at 37 477.5 cm^{-1}. The weaker features to the blue of the origin are due to methyl torsions. Specific assignments are given in Table II.

seen to occur at 37 477.5 cm^{-1} with weaker features at 16.2, 54.0, and 77.5 cm^{-1} to higher energy. Contrary to the results reported by Ito et al.,[14] none of these weak features varies in intensity upon changing the helium backing pressure from 20–130 psig. The use of argon, nitrogen, and 1% CF_4 in 100 psig of helium as carrier gases also did not alter the intensities of these features.

Figure 4 shows the dispersed emission spectrum of jet-cooled toluene excited at 37 477.5 cm^{-1}. A series of weak features, spaced at 17, 49, 80, and 128 cm^{-1} to the red of the origin, is apparent.

The TOFMS and DE spectrum for toluene are fit by the energy levels listed in Table I, using model parameters $B = 5.2$ cm^{-1} and $V_6 = 10$ cm^{-1} in the ground state, and $B = 5.2$ and $V_6 = 25$ cm^{-1} in the excited state. The calculated zero-point energies for S_0 and S_1 are 4.9 and 12.1 cm^{-1}, respectively. The features in the TOFMS at 16.2, 54.0, and 77.5 cm^{-1} closely match the energies for the $1e'' \rightarrow 2e'$, $0a_1' \rightarrow 3a_1''$, and $1e'' \rightarrow 4e'$ transitions. The $0a_1' \rightarrow 3a_2''$ transition is not observed in agreement with the group theoretically derived selection rules stated above.

Table II lists the allowed transitions, and their calculated and observed energies, for the ground and first excited states of toluene. The spacings of the features observed in the DE spectrum closely match the calculated energies listed in Table II. The low barrier of $V_6 = 10$ cm^{-1} in the ground state is consistent with microwave studies performed by Rudolph et al.[15] on toluene in which a barrier to rotation of the methyl rotor of 4.9 cm^{-1} was reported.

Given the above assignments, the features at 16.2 and 77.5 cm^{-1} in the TOFMS are hot bands and might therefore be expected to show a temperature effect. The (a) and (e) methyl rotor states, however, possess different nuclear spin states for which interconversion is strongly forbidden, and thus the hot band features at 16.2 and 77.5 cm^{-1} can never
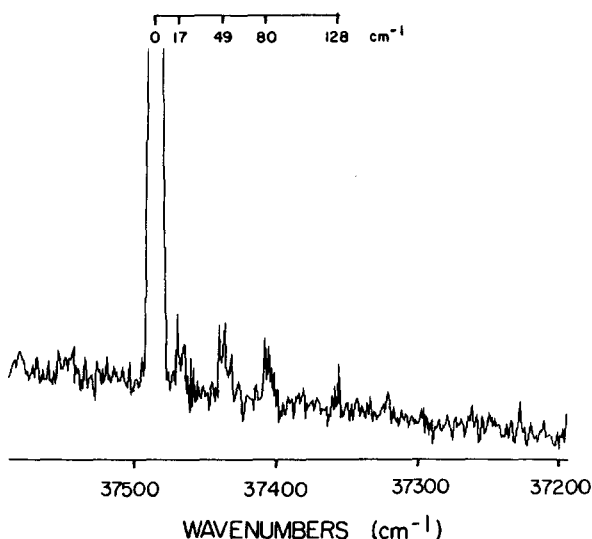
be cooled completely from the spectrum. Two different types of toluene molecules exist in the cooled beam: those in the $0a_1'$ and those in the $1e''$ internal rotational states.

The low barrier to rotation about the $C_{ipso}-C_\alpha$ bond in S_0 as determined by the TOFMS and DE study is also found in the EFF calculations. Indeed, the MOMM steric energies for the different $C_{ipso}-C_\alpha$ rotomers of toluene are essentially the same within 0.02 kcal/mol (~ 7 cm^{-1}), indicative of a free rotor system.

In summary the methyl rotor experiences only a small (~ 17 cm^{-1}) increase in the barrier to rotation when toluene is excited from S_0 to S_1, and is essentially freely rotating in both states.

B. p-Xylene

The TOFMS of jet-cooled p-xylene is presented in Fig. 5. While the origin occurs at 36 732.8 cm^{-1} the spectrum is similar to that observed for toluene (Fig. 3) in that features are found at 15.5, 54.3, and 78.1 cm^{-1} to higher energy of the origin band. Additional weak features not present in the toluene spectrum occur at 40.5, 72.0, and 109.5 cm^{-1}. As in toluene, none of the peak intensities show any dependence on the backing pressure of the nozzle (20–140 psig He).

The energy levels for the combined total internal rota-

TABLE I. Internal rotational levels for toluene in the S_0 and S_1 states.

Ground state S_0[a]		Excited state S_1[b]	
Level	Energy (cm^{-1})	Level	Energy (cm^{-1})
$0a_1'$	0	$0a_1'$	0
$1e''$	5.19	$1e''$	5.15
$2e'$	20.78	$2e'$	20.60
$3a_2''$	45.56	$3a_2''$	40.97
$3a_1''$	48.06	$3a_1''$	53.47
$4e'$	83.23	$4e'$	84.24
$5e''$	128.80	$5e''$	130.73

[a] $B = 5.2$ cm^{-1}, $V_3 = 0$ cm^{-1}, $V_6 = 10$ cm^{-1}.
[b] $B = 5.2$ cm^{-1}, $V_3 = 0$ cm^{-1}, $V_6 = 25$ cm^{-1}.

FIG. 4. DE spectrum of the 0_0^0 region of toluene (resolution of 15 cm^{-1}) obtained by pumping the origin at 37 477.5 cm^{-1}. The weak features to lower energy of the origin are again due to methyl torsions. Specific assignments are given in Table II.

TABLE II. Energies of allowed transitions between internal rotational levels in the S_0 and S_1 states for toluene.

Transition $(S_1 \rightarrow S_0)$	Calculated E (cm^{-1})	Observed E (cm^{-1}) by DE
$0a_1' \rightarrow 0a_1'$	0	0
$0a_1' \rightarrow 3a_1''$	48.06	49
$1e'' \rightarrow 1e''$	0	0
$1e'' \rightarrow 2e'$	15.63	17
$1e'' \rightarrow 4e'$	78.08	80
$1e'' \rightarrow 5e''$	123.65	128

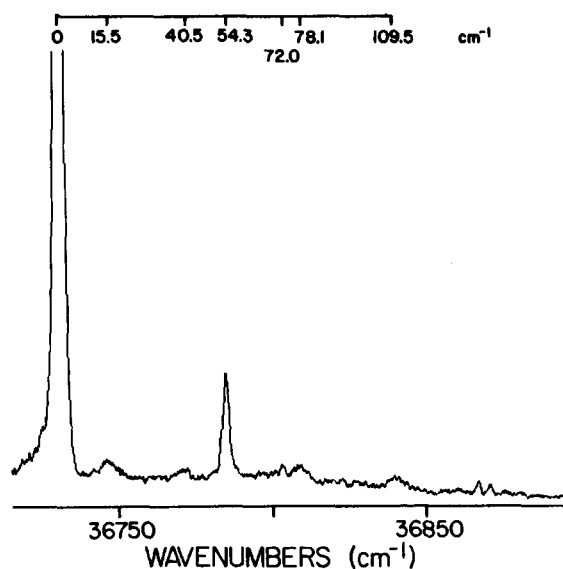| Transition $(S_0 \rightarrow S_1)$	Calculated E (cm^{-1})	Observed E (cm^{-1}) by TOFMS
$0a_1' \rightarrow 0a_1'$	0	0
$0a_1' \rightarrow 3a_1''$	53.47	54.0
$1e'' \rightarrow 1e''$	0	0
$1e'' \rightarrow 2e'$	15.41	16.2
$1e'' \rightarrow 4e'$	79.05	77.5

FIG. 5. One-color TOFMS of the 0_0^0 region of p-xylene. The origin occurs at 36 732.8 cm^{-1}. The weak features to higher energy of the origin are due to methyl torsions. Note that several features in the spectrum coincide with those observed for toluene (Fig. 3), suggesting similarities in the potentials for methyl rotation in both molecules. Peak assignments are given in Table IV.

tional states of both methyl rotors in p-xylene are obtained by treating the rotors as noninteracting. The resultant energy levels, listed in Table III, simply represent all possible combinations of internal rotational states of a one-dimensional rotor with itself. Thus, for example, the excited state energy levels in Table III represent the combination of states of two rotors which individually behave as the toluene methyl rotor does in its S_1 state.

The simplest method for symmetry labeling the energy

TABLE III. Internal rotational levels for p-xylene in the S_0 and S_1 states.

Ground state S_0^a		Excited state S_1^b	
Level	Energy (cm^{-1})	Level	Energy (cm^{-1})
$0a_1'0a_1'$	0	$0a_1'0a_1'$	0
$0a_1'1e''$	5.19	$0a_1'1e''$	5.15
$1e''1e''$	10.39	$1e''1e''$	10.30
$0a_1'2e'$	20.78	$0a_1'2e'$	20.60
$1e''2e'$	25.98	$1e''2e'$	25.75
$2e'2e'$	41.57	$0a_1'3a_2''$	41.00
$0a_1'3a_2''$	45.56	$2e'2e'$	41.20
$0a_1'3a_1''$	48.06	$1e''3a_2''$	46.15
$1e''3a_2''$	50.76	$0a_1'3a_1''$	53.47
$1e''3a_1''$	53.26	$1e''3a_1''$	58.62
$2e'3a_2''$	66.34	$2e'3a_2''$	61.60
$2e'3a_1''$	68.84	$2e'3a_1''$	74.07
$0a_1'4e'$	83.23	$3a_2''3a_2''$	82.00
$1e''4e'$	88.43	$0a_1'4e'$	84.24
$3a_2''3a_2''$	91.12	$1e''4e'$	89.39
$3a_2''3a_1''$	93.62	$3a_2''3a_1''$	94.57
$3a_1''3a_1''$	96.12	$2e'4e'$	104.84
$2e'4e'$	104.02	$3a_1''3a_1''$	106.94

$^a B = 5.2$ cm^{-1}, $V_3 = 0$ cm^{-1}, $V_6 = 10$ cm^{-1}.
$^b B = 5.2$ cm^{-1}, $V_3 = 0$ cm^{-1}, $V_6 = 25$ cm^{-1}.

levels for p-xylene is to consider the internal rotational states of each rotor separately, and thus use the symmetry labels and selection rules for toluene. A p-xylene molecule with one rotor in its $0a_1'$ state and the other in its $1e''$ state is thereby said to be in the $0a_1'1e''$ state. The molecular symmetry group for p-xylene is G_{72}, and the fourfold degenerate $0a_1'1e''$ energy level is labeled $1G$ in the molecular symmetry group. A $0a_1'0a_1' \rightarrow 1e''0a_1'$ transition is thus an $A_1 \rightarrow G$ transition, which is symmetry forbidden. The $0a_1'1e''$ form of symmetry labeling is used here because it clarifies the levels of each individual methyl rotor and reveals which transitions take place on which methyl rotor. The approximation of separate noninteracting rotors is assumed for this discussion.

Since a two rotor system (e.g., xylenes) has many more levels than a one rotor system (e.g., toluene), the TOFMS of p-xylene should have many more features than that of toluene. Table IV lists the allowed transitions, their calculated and observed energies, and the fitted parameters. The approximation of two completely uncoupled, independent rotors for p-xylene appears to be a good one since this model matches the observed spectrum well. Each methyl rotor individually experiences a potential barrier of $V_6 = 10$ cm^{-1} and $V_6 = 25$ cm^{-1} in the S_0 and S_1 states, respectively, as in toluene. The calculated zero point energies for S_0 and S_1 are the same as for toluene (4.9 and 12.1 cm^{-1}, respectively). This is largely consistent with previous results which indicate that the rotors in p-xylene are nearly free.[16]

EFF calculations performed on p-xylene show that both the heats of formation (ΔH_f^0) and steric energies can be directly related to the ΔH_f^0 and steric energies of benzene and toluene by linear free energy relationships, i.e., by additivity of energies.[17] This supports the notion that the methyl groups of p-xylene are noninteractive.

C. m-Xylene

Figure 6 shows the TOFMS of jet-cooled m-xylene. In contrast to the other compounds presented thus far, m-xylene displays an intense triplet feature at the origin region, with components at 36 949.3, 36 952.6, and 36 956.3 cm^{-1}.

TABLE IV. Energies of allowed transitions between internal rotational levels in the S_0 and S_1 states of p-xylene.

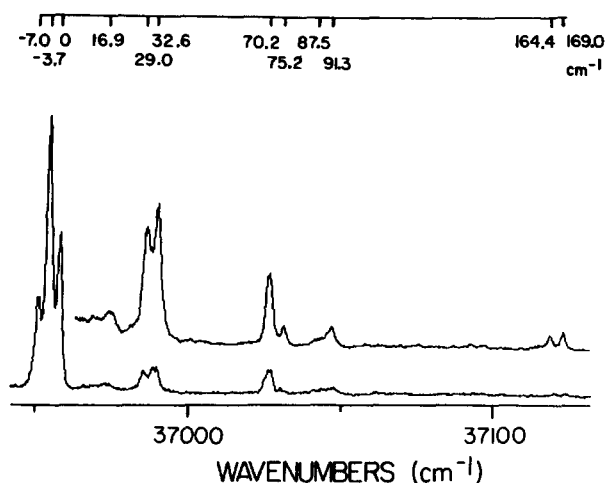| Transition ($S_0 \rightarrow S_1$)	Calculated E (cm^{-1})	Observed E (cm^{-1}) by TOFMS
$0a_1'0a_1' \rightarrow 0a_1'0a_1'$	0	0
$0a_1'0a_1' \rightarrow 0a_1'3a_1''$	53.47	54.3
$0a_1'0a_1' \rightarrow 3a_1''3a_1''$	106.94	109.5
$1e''0a_1' \rightarrow 1e''0a_1'$	-0.04	0
$1e''0a_1' \rightarrow 2e'0a_1'$	15.41	15.5
$1e''0a_1' \rightarrow 1e''3a_1''$	53.43	54.3
$1e''0a_1' \rightarrow 2e'3a_1''$	68.88	72.0
$1e''0a_1' \rightarrow 4e'0a_1'$	79.05	78.1
$1e''1e'' \rightarrow 1e''1e''$	-0.09	0
$1e''1e'' \rightarrow 2e'1e''$	15.36	15.5
$1e''1e'' \rightarrow 2e'2e'$	30.81	...
$1e''1e'' \rightarrow 4e'1e''$	79.00	78.1
$1e''1e'' \rightarrow 4e'2e'$	94.45	...

FIG. 6. One-color TOFMS of the 0_0^0 region of *m*-xylene. The origin occurs at 36 956.3 cm^{-1}. The two features at 3.7 and 7.0 cm^{-1} to lower energy of the origin are due to methyl torsions, and their positions are indicative of differences in the potential barrier to methyl rotation in S_1 and S_0. The weak features to higher energy of the origin are also due to methyl torsions. Assignments are given in Table VI(b).

FIG. 7. DE spectra of the 0_0^0 region of *m*-xylene (resolution 11.4 cm^{-1}) obtained by pumping at (a) 36 949.3 cm^{-1}, (b) 36 952.6 cm^{-1}, and (c) 36 956.3 cm^{-1}. Assignments are given in Table VI(a).

A number of additional features, several of which appear to be doublets, are seen to higher energy of the 0_0^0 triplet.

The DE spectra obtained by exciting each of the components of the origin triplet are presented in Figs. 7(a)–7(c). While the spectra in Figs. 7(a) and 7(b) both reveal transitions near 16 and 80 cm^{-1} to the red of their respective origins, Fig. 7(c) displays peaks only at $\sim$54 and 102 cm^{-1} from the origin. *m*-Xylene is again a double rotor system, so that the same symmetry lables used for the internal rotational levels of *p*-xylene are used here. The methyl rotors are once again assumed to be noninteracting. The features at 54 and 102 cm^{-1} in Fig. 7(c) are assigned to be the $0a_1'0a_1' \rightarrow 0a_1'3a_1''$ and $0a_1'0a_1' \rightarrow 3a_1''3a_1''$ transitions, respectively, and the transition at 36 956.3 cm^{-1} in the TOFMS (Fig. 6) is therefore taken to be the true origin ($0a_1'0a_1' \rightarrow 0a_1'0a_1'$) of the TOFMS spectrum.

The different nuclear spin states associated with the *a* and *e* levels result in hot bands which cannot be depopulated by normal cooling techniques. For the xylenes, the molecular jet contains three different types of molecules which cannot interconvert; those in the $0a_1'0a_1'$, $1e''0a_1'$, and $1e''1e''$ internal rotational levels. The relative statistical weights for these states are 1:2:1, respectively. This ratio coincides with the observed relative intensities in Fig. 6.

The energy levels for internal rotation of the methyl rotors in the ground state of *m*-xylene are listed in Table V. Table VI(a) lists the allowed calculated and observed DE transition energies for the ground state. The fit is good indicating that the methyl rotors in the ground state are subject to a low barrier to rotation ($B = 5.2$ cm^{-1}, $V_3 = 0$ cm^{-1}, $V_6 = 25$ cm^{-1}, zero-point energy $= 12.1$ cm^{-1}), which is again consistent with earlier results on this molecule.[16]

To consider methyl rotation in the S_1 excited state, the TOFMS must be completely understood. Several facts become apparent upon examination of Fig. 6. First, the features at 36 949.3 and 36 952.6 cm^{-1} are red shifted by 7 and

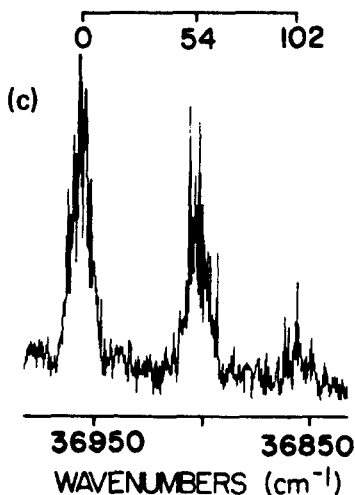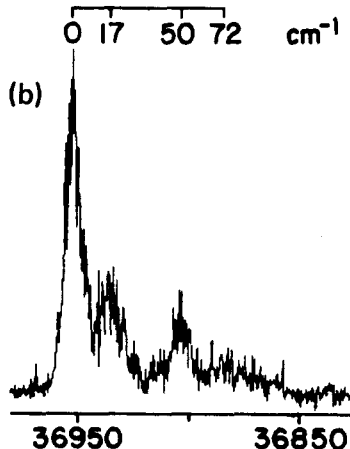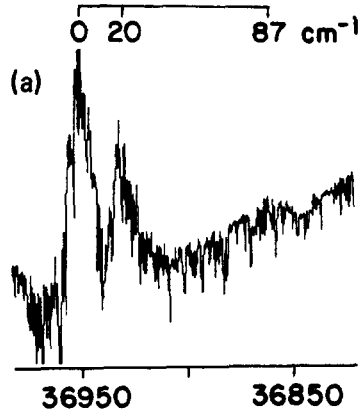3.7 cm^{-1}, respectively, from the origin at 36 956.3 cm^{-1}. This requires that the energy level spacings between the $0a_1'0a_1'$, $1e''0a_1'$, and $1e''1e''$ levels in the excited state be *smaller* than in the ground state; this can only happen if the barrier to rotation of the methyl group increases in S_1 with respect to S_0. Second, the absence of a peak near $\sim$54 cm^{-1}, corresponding to the $0a_1'0a_1' \rightarrow 0a_1'3a_1''$ transition of a nearly free rotor also suggests the presence of a sizable barrier to rotation in S_1.

TABLE V. Internal rotational levels for *m*-xylene in the S_0 and S_1 states.

Ground state $S_0{}^a$		Excited state $S_1{}^b$	
Level	Energy (cm^{-1})	Level	Energy (cm^{-1})
$0a_1'0a_1'$	0	$0a_1'0a_1'$	0
$0a_1'1e''$	5.15	$0a_1'1e''$	1.66
$1e''1e''$	10.30	$1e''1e''$	3.31
$0a_1'2e'$	20.60	$0a_1'2e'$	37.64
$1e''2e'$	25.75	$1e''2e'$	39.30
$0a_1'3a_2''$	41.00	$0a_1'3a_2''$	48.87
$2e'2e'$	41.20	$1e''3a_2''$	50.53
$1e''3a_2''$	46.15	$0a_1'3a_1''$	74.77
$0a_1'3a_1''$	53.47	$2e'2e'$	75.28
$1e''3a_1''$	58.62	$1e''3a_1''$	76.43
$2e'3a_2''$	61.60	$2e'3a_2''$	86.51
$2e'3a_1''$	74.07	$3a_2''3a_2''$	97.74
$3a_2''3a_2''$	82.00	$0a_1'4e'$	99.32
$0a_1'4e'$	84.24	$1e''4e'$	100.98
$1e''4e'$	89.39	$2e'3a_1''$	112.41
$3a_2''3a_1''$	94.57	$3a_1''3a_1''$	123.64
$2e'4e'$	104.84	$2e'4e'$	136.96
$3a_1''3a_1''$	106.94	$0a_1'5e''$	144.87
		$1e''5e''$	146.53
		$3a_2''4e'$	148.19
		$3a_1''3a_1''$	149.54
		$3a_1''4e'$	174.09
		$2e'5e''$	182.51

$^aB = 5.2$ cm^{-1}, $V_3 = 0$ cm^{-1}, $V_6 = 25$ cm^{-1}.
$^bB = 5.2$ cm^{-1}, $V_3 = 81$ cm^{-1}, $V_6 = -30$ cm^{-1}.

Table V lists the energy levels for internal rotation in the S_1 excited state for $B = 5.2$ cm^{-1}, $V_3 = 81$ cm^{-1}, and $V_6 = -30$ cm^{-1}. The calculated zero-point energy is 13.1 cm^{-1}. Table VI(b) lists the allowed transitions and calculated and observed TOFMS transition energies. The fit of the calculated values to the spectrum is quite good and again justifies the assumption that the two methyl groups are noninteracting.

As is the case for *p*-xylene, EFF calculations performed on *m*-xylene indicate additivity in both energy (ΔH_f^0 and SE) and structure, when data for benzene and toluene are compared with data for *m*-xylene. This again suggests that the two methyl groups of *m*-xylene are acting independently of each other[17] in S_0, and supports the experimental conclusion.

D. *o*-Xylene

The TOFMS of jet-cooled *o*-xylene is depicted in Fig. 8. The outstanding feature of this spectrum, apart from the single origin at 37 313.3 cm^{-1}, is the large featureless expanse from the origin to 37 421.3 cm^{-1}, at which energy several weak features begin to appear. The lack of features within the first 100 cm^{-1} of the origin is indicative of a strongly hindered methyl rotor. Steric hindrance should not be unexpected in the *o*-xylene molecule.

The close proximity of the methyl rotors in *o*-xylene further requires the consideration of both kinetic and potential cross terms between the methyl rotors in the Hamiltonian. Indeed, the spectrum in Fig. 8 cannot be fit using sim-

TABLE VI. Energies of allowed transitions between internal rotational levels in the S_1 and S_0 state of *m*-xylene.

(A)

Transition ($S_1 \rightarrow S_0$)	Calculated E (cm^{-1})	Observed E (cm^{-1}) by DE
$0a_1'0a_1' \rightarrow 0a_1'0a_1'$	0	0
$0a_1'0a_1' \rightarrow 0a_1'3a_1''$	53.47	54
$0a_1'0a_1' \rightarrow 3a_1''3a_1''$	106.94	102
$1e''0a_1' \rightarrow 1e''0a_1'$	0	0
$1e''0a_1' \rightarrow 2e'0a_1'$	15.45	17
$1e''0a_1' \rightarrow 1e''3a_1''$	53.47	50
$1e''0a_1' \rightarrow 2e'3a_1''$	68.92	72
$1e''0a_1' \rightarrow 0a'4e_1'$	79.09	$\cdots$
$1e''1e'' \rightarrow 1e''1e''$	0	0
$1e''1e'' \rightarrow 2e''1e'$	15.45	20
$1e''1e'' \rightarrow 2e'2e'$	30.90	$\cdots$
$1e''1e'' \rightarrow 1e''4e'$	79.09	87
$1e''1e'' \rightarrow 2e'4e'$	94.54	87

(B)

| Transition ($S_0 \rightarrow S_1$)	Calculated E (cm^{-1})	Observed E (cm^{-1}) by TOFMS
$0a_1'0a_1' \rightarrow 0a_1'0a_1'$	0	0
$0a_1'0a_1' \rightarrow 0a_1'3a_1''$	74.77	75.2
$0a_1'0a_1' \rightarrow 3a_1''3a_1''$	149.54	$\cdots$
$1e''0a_1' \rightarrow 1e''0a_1'$	-3.49	-3.7
$1e''0a_1' \rightarrow 2e'0a_1'$	32.49	32.6
$1e''0a_1' \rightarrow 1e''3a_1''$	71.28	70.2
$1e''0a_1' \rightarrow 2e'3a_1''$	107.26	$\cdots$
$1e''0a_1' \rightarrow 4e'0a_1'$	94.17	91.3
$1e''0a_1' \rightarrow 5e''0a_1'$	139.72	132.9
$1e''0a_1' \rightarrow 4e'3a_1''$	168.94	164.4
$1e''1e'' \rightarrow 1e''1e''$	-6.99	-7.0
$1e''1e'' \rightarrow 2e'1e''$	29.00	29.0
$1e''1e'' \rightarrow 2e'2e'$	64.98	$\cdots$
$1e''1e'' \rightarrow 4e'1e''$	90.68	87.5
$1e''1e'' \rightarrow 4e'2e'$	126.66	$\cdots$
$1e''1e'' \rightarrow 5e''1e''$	136.23	141.9
$1e''1e'' \rightarrow 5e''2e'$	172.21	169.0
$2e'0a' \rightarrow 2e'0a'$	17.04	16.9
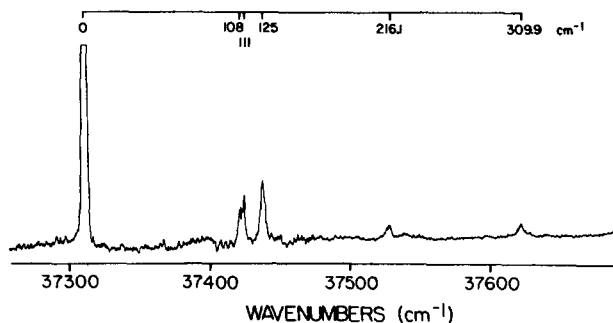
FIG. 8. One-color TOFMS of the 0_0^0 region of *o*-xylene. The origin occurs at 37 313.3 cm^{-1}. Note the absence of peaks within the first 100 cm^{-1} of the origin. Such spacing between the 0_0^0 transition and the first methyl torsional modes is indicative of a large (> 100 cm^{-1}) potential barrier to methyl rotation in the excited state S_1. Peak assignments are given in Table VIII(b).

ply V_3 and V_6 potential terms. A large V_6 potential would be physically inappropriate to describe the potential that the methyl rotors experience, while a large V_3 potential creates tightly bunched groups of levels (only a few wave numbers apart) with large (~ 50–100 cm^{-1}) spacings between groups. A V_3 potential large enough to shift, for example, the $3a_1''0a_1'$ level to ~ 125 cm^{-1} would not place any other levels near 110 cm^{-1}.

If the band at 125 cm^{-1} in the TOFMS is due to the $0a_1'0a_1' \rightarrow 0a_1'3a_1''$ transition (since this peak is the most intense and the $0a_1'0a_1' \rightarrow 0a_1'3a_1''$ is observed in toluene and *p*-xylene to be the most intense), then a V_3' potential cross term which splits the doubly degenerate $0a_1'3a_1''$ level is required to place accessible energy levels near 110 cm^{-1}. A parameter set with $B = 5.5$ cm^{-1}, $V_3 = 166$ cm^{-1}, $V_3' = -25$ cm^{-1}, and $\chi = 0.72$ yields the levels listed in Table VII for the S_1 state of *o*-xylene. A zero-point energy of 101.9 cm^{-1} is obtained. Table VIII lists the calculated and observed transition energies for S_1. The use of cross kinetic and potential terms for S_1 is reasonable given the close proximity of the methyl groups: this is the only molecule in the series for which a coupled rotor model is required to account for the experimental observations.

The DE spectrum exciting the origin band of *o*-xylene is presented in Fig. 9. As in the TOFMS, the wide spacings between the peaks in the spectrum dictate a large potential barrier to methyl rotation. The feature at 250 cm^{-1} is as-

TABLE VIII. Energies of allowed transitions between internal rotational levels in the S_0 and S_1 states of *o*-xylene.

(A)

Transition ($S_1 \rightarrow S_0$)	Calculated E (cm^{-1})	Observed E (cm^{-1}) by DE
$0a_1'0a_1' \rightarrow 0a_1'0a_1'$	0	0
$0a_1'0a_1' \rightarrow 0a_1'3a_1''$	246.21	249
$0a_1'0a_1' \rightarrow 0a_1'6a_2'$	354.55	···
$0a_1'0a_1' \rightarrow 0a_1'6a_1'$	383.30	···
$0a_1'1e'' \rightarrow 0a_1'1e''$	0.00	0
$0a_1'1e'' \rightarrow 0a_1'2e'$	134.54	134
$0a_1'1e'' \rightarrow 3a_1''1e''$	246.22	249
$0a_1'1e'' \rightarrow 0a_1'4e'$	249.82	249
$0a_1'1e'' \rightarrow 0a_1'5e''$	329.64	327
$0a_1'1e'' \rightarrow 6a_2'1e''$	354.56	···
$0a_1'1e'' \rightarrow 3a_1''2e'$	380.76	···
$0a_1'1e'' \rightarrow 6a_1'1e''$	383.30	···
$1e''1e'' \rightarrow 1e''1e''$	0.00	0
$1e''1e'' \rightarrow 1e''2e'$	134.55	134
$1e''1e'' \rightarrow 1e''4e'$	249.83	249
$1e''1e'' \rightarrow 2e'2e'$	269.09	···
$1e''1e'' \rightarrow 1e''5e''$	329.65	327

(B)

Transition ($S_0 \rightarrow S_1$)	Calculated E (cm^{-1})	Observed E (cm^{-1}) by TOFMS
$0a_1'0a_1' \rightarrow 0a_1'0a_1'$	0.00	0.0
$0a_1'1e'' \rightarrow 0a_1'1e''$	0.15	0.0
$1e''1e'' \rightarrow 1e''1e''$	0.29	0.0
$1e''1e'' \rightarrow 1e''2e'$	60.70	···
$1e''1e'' \rightarrow 1e''2e'$	60.73	···
$0a_1'1e'' \rightarrow 0a_1'2e'$	62.30	···
$1e''1e'' \rightarrow 1e''2e'$	82.90	···
$1e''1e'' \rightarrow 1e''2e'$	88.30	···
$0a_1'0a_1' \rightarrow 0a_1'3a_1''$	108.04	108.0
$0a_1'1e'' \rightarrow 3a_1''1e''$	111.76	111.0
$1e''1e'' \rightarrow 1e''4e'$	119.57	···
$1e''1e'' \rightarrow 1e''4e'$	120.11	···
$0a_1'0a_1' \rightarrow 0a_1'3a_1''$	124.83	125.0
$0a_1'1e'' \rightarrow 0a_1'4e'$	133.65	···
$0a_1'0a_1' \rightarrow 0a_1'6a_2'$	215.37	···
$0a_1'0a_1' \rightarrow 0a_1'6a_2'$	216.50	···
$0a_1'0a_1' \rightarrow 0a_1'6a_1'$	218.16	216.1
$0a_1'1e'' \rightarrow 6a_2'1e''$	219.01	···
$0a_1'0a_1' \rightarrow 0a_1'6a_1'$	219.83	···
$0a_1'1e'' \rightarrow 6a_1'1e''$	221.07	···

TABLE VII. Internal rotational levels of *o*-xylene in the S_0 and S_1 states.

Ground state S_0 [a]		Excited state S_1 [b]	
Level	Energy (cm^{-1})	Level	Energy (cm^{-1})
$0a_1'0a_1'$	0	$0a_1'0a_1'$	0
$0a_1'1e''$	0.00	$0a_1'1e''$	0.15
$1e''1e''$	0.01	$1e''1e''$	0.30
$0a_1'2e'$	134.54	$1e''2e'$	60.71
$1e''2e'$	134.55	$1e''2e'$	60.74
$0a_1'3a_2''$	134.78	$0a_1'2e'$	62.30
$1e''3a_2''$	134.78	$0a_1'3a_2'$	64.07
$0a_1'3a_1''$	246.21	$1e''2e'$	87.91
$1e''3a_1''$	246.22	$1e''2e'$	88.31
$0a_1'4e'$	249.82	$1e''3a_2''$	89.55
$1e''4e'$	249.83	$0a_1'3a_2''$	91.12
$2e'2e'$	269.09	$0a_1'3a_1''$	108.04
$2e'3a_2''$	269.32	$1e''3a_1''$	111.76
$3a_2''3a_2''$	269.55	$1e''4e'$	119.58
$0a_1'5e''$	329.64	$1e''4e'$	120.12
$1e''5e''$	329.65	$0a_1'3a_1''$	124.83
$0a_1'6a_2'$	354.55	$0a_1'4e'$	133.65
$1e''6a_2'$	354.56	⋮	
$2e'3a_1''$	380.76	$0a_1'6a_2'$	215.37
$3a_2''3a_1''$	380.99	$0a_1'6a_2'$	216.50
$0a_1'6a_1'$	383.30	$0a_1'6a_1'$	218.16
$1e''6a_1'$	383.30	$1e''6a_2'$	219.01
		$0a_1'6a_1'$	219.83
		$1e''6a_1'$	221.07

[a] $B = 5.2$ cm^{-1}, $V_3 = 425$ cm^{-1}, $V_6 = 18$ cm^{-1}.
[b] $B = 5.2$ cm^{-1}, $V_3 = 166$ cm^{-1}, $V_3' = -25$ cm^{-1}, $V_6 = 0$ cm^{-1}, $\chi = 0.72$ cm^{-1}.

signed to be in part due to the $0a_1'0a_1' \rightarrow 0a_1'3a_1''$ transition, and thus the barrier in the ground state is even larger than that for the excited state. A potential barrier of $V_3 = 425$ cm^{-1} and $V_6 = 18$ cm^{-1}, with $B = 5.2$ cm^{-1} gives energy levels (see Table VII) which correspond well with the peaks in Fig. 9. The resultant zero-point energy is 144.0 cm^{-1}. The observed and calculated transition energies are listed in Table VIII(a). Neither a potential cross term V_3' nor a cross kinetic energy term χ is needed to fit the *o*-xylene DE spectrum. The molecular orbitals on the methyl groups in the S_1 excited state are larger, more diffuse, and have a larger electron density than those in the ground state: the two methyl groups must therefore interact much more strongly in the
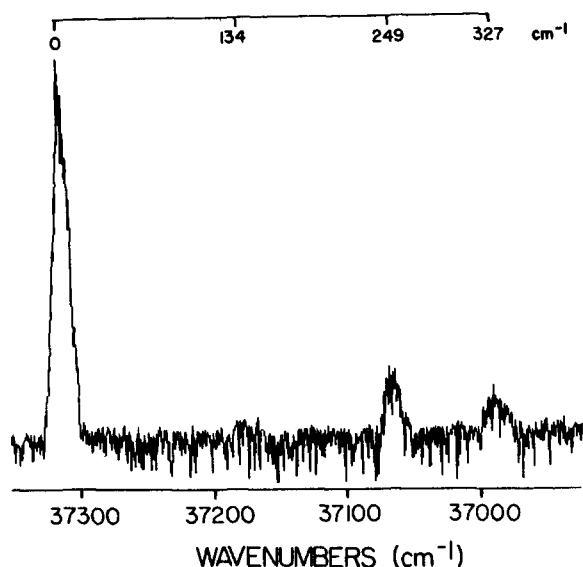
FIG. 9. DE spectrum of the 0_0^0 region of *o*-xylene (resolution 15.2 cm^{-1}) obtained by pumping the origin at 37 313.3 cm^{-1}. The wide spacings between peaks in the spectrum is indicative of a large (> 100 cm^{-1}) potential barrier to methyl rotation in the ground state S_0. Peak assignments are given in Table VIII(a).

excited state than in the ground state. The approximation of two noninteracting methyl rotors appears to fail for the S_1 state of *o*-xylene but may still be considered reasonable for the ground state.

EFF calculations on *o*-xylene confirm the above conclusions for S_0. Interconversion from one "gear clashed" conformation **1** (Fig. 10) to another has a definite energy barrier
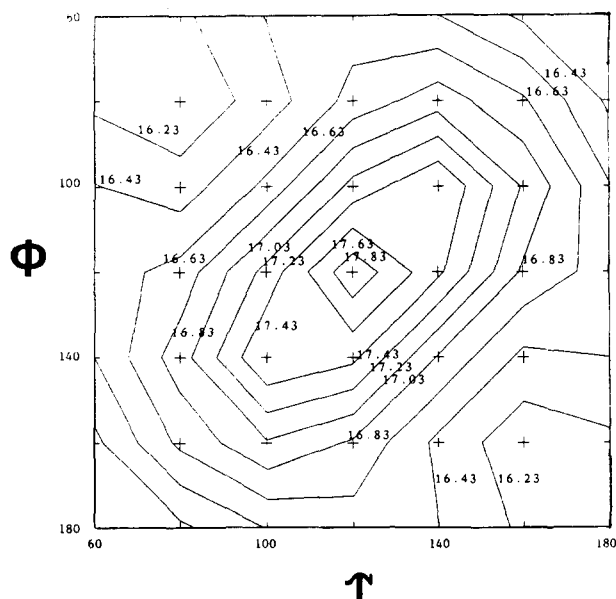

FIG. 10. MOMM-85 calculated steric energy contour for methyl group rotation [about ϕ and τ, where ϕ and τ = torsion ($C_{ipso'}$–C_{ispo}–C_α–H_α) cf. **1**] in *o*-xylene. The maximum in the center of the figure corresponds to hydrogen atoms from each methyl group lying in the plane of the ring pointed directly at each other. The minima in the figure occur at each corner and correspond to a hydrogen atom of each methyl group pointing away from the other methyl group, and being in the plane of the ring. The lowest energy pathways which connect the minima are along the borders of the figure, indicating that the interconversion from one minimum to another can be accomplished in a noncoupled motion.

with a maximum energy conformation **2**, in contrast with the situation for rotation of the methyl group to toluene (and in *m*- and *p*-xylenes) for which the EFF calculations predicted free rotation without any definitive energy maximum. As can be seen from Fig. 10, interconversion of one stable conformation into another can best occur with an uncoupled motion of one methyl rotor relative to the other, i.e., movement around the periphery of the energy maximum in Fig. 10.[18] Recent *ab initio* MO calculations on toluene and *o*-xylene,[19] published following completion of our studies, confirm these MOMM-85 calculations. In addition, the experimental and theoretically calculated heat of formation of *m*- and *p*-xylene is ~0.3 kcal/mol less than that of *o*-xylene,[20] and the steric energies show that *o*-xylene is more strained as well. Thus, EFF calculations predict that the methyl rotational motion in *o*-xylene is somewhat different than that for toluene and *m*- and *p*-xylenes, consistent with the experimental observations.

1

2
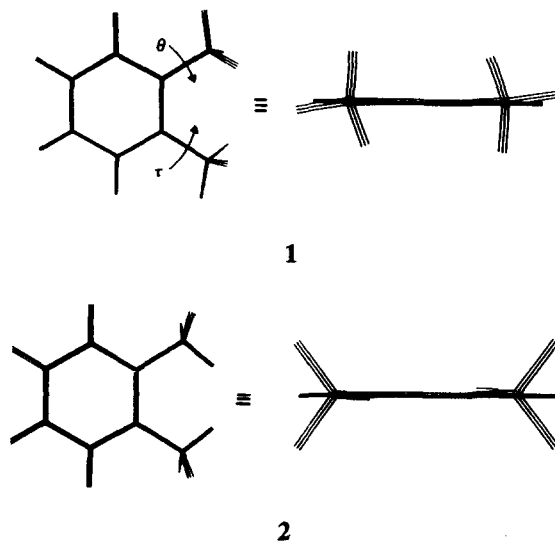
The results for *o*-xylene compare well with those obtained by analyses of NMR,[21,22] microwave,[23] and heat capacity[16,24,25] data for this molecule. These studies generally conclude or assume that the methyl rotors are uncoupled in S_0 with a potential barrier height of 500–700 cm^{-1}. For S_1, room temperature optical absorption data[26] analyzed in a similar manner to those discussed above imply a barrier of 200–300 cm^{-1} for uncoupled methyl groups. The coupling of the methyl groups could not be evaluated in these previous studies.

V. SUMMARY AND CONCLUSION

The results of this work demonstrate that the steric effects of methyl rotors are small for methyl–ring interactions as well as for methyl–methyl interactions for nonadjacent methyl groups. In toluene, a very small rotational barrier is encountered in both S_0 and S_1. For the xylenes, the heights of the methyl rotor potential barriers decrease in the order ortho > meta > para and can be attributed simply to the increased steric hindrance between rotors in the series. In addition, the systems studied reveal an increase in the barrier to rotation upon electronic excitation, although the notion of "barrier height" may be complicated by cross kinetic and

potential terms in the Hamiltonian. This heightened steric effect in S_1 can be explained by the larger, more diffuse molecular orbitals in the excited state (both on the ring and on the methyl groups, in general) which make the methyl groups more susceptible to steric hindrance. Hyperconjugation may also play a role in the excited state steric barrier to rotation: the ring structure may be extended to involve the methyl carbons in the excited state.

The approximation of noninteracting methyl rotors seems to be valid for all three xylene isomers in the ground state and for meta and para isomers in the excited S_1 state. Both potential and kinetic cross terms are necessary to describe the dynamics of the methyl rotors in the S_1 state of *o*-xylene. In this last case, the inclusion of both potential and kinetic cross terms in the Hamiltonian represents a tendency towards "cogwheeling" or "gearing" of the rotors.[1,27] Such coupling has been postulated to occur for *o*-xylene in the ground electronic state, although experimental evidence that the rotors are coupled in that state is missing. Our results indicate that coupling between the rotors is negligible for the S_0 state but do reveal a strong coupling of the two methyl rotors in S_1 of *o*-xylene.

For all four molecules studied, in both the TOFMS and DE spectra, the intensities of the torsional features fall off rapidly from the origin. This implies that the best Franck–Condon overlap lies on or near the origin and that little change in the equilibrium orientation of the methyl groups occurs upon electronic excitation. (This contrasts with the fluorotoluenes for which, for example, the ortho isomer at equilibrium experiences a 60° methyl group rotation upon excitation.[6]) We have therefore foregone a detailed analysis of the transition intensities observed.

Some general intensity propensity rules are readily derived from our data on toluene and the xylenes: (1) the most intense transitions in the spectra, aside from the origin transitions, involve the rotor transition $0a_1' \rightarrow 3a_1''$; and (2) double rotor transitions $(0a_1'0a_1' \rightarrow 3a_1''3a_1'')$ are inherently weak.

The approach of treating the methyl group as a one-dimensional rigid rotor and of fitting the resulting internal rotational states to observed features in the TOFMS and DE spectra of toluene and the xylenes works well. For each species, physically realistic values of a limited number of parameters are used to produce calculated spectra which closely match those observed experimentally. Comparison of the potential barrier parameters obtained in this manner with those obtained by other means reveals that the integrated techniques employed in this work can produce accurate values of these parameters. Even in instances for which variation of many parameters is required to fit the data, implying that the chosen set of parameter values may not be unique, a clear picture of the torsional interaction is still generated, as evidenced by the *o*-xylene fits. Thus, this method may be utilized to study more complex systems for which intersub-stituent interactions may be more complicated. This is demonstrated in the succeeding paper for the *n*-propyltoluenes.[7]

Finally, the EFF-MOMM calculations give results consistent with the ground state barriers and rotational models and appear to be qualitatively reliable.

ACKNOWLEDGMENTS

[1] S. Sternhell, in *Dynamic Nuclear Magnetic Resonance Spectroscopy*, edited by L. M. Jackman and F. A. Cotton (Academic, New York, 1975); M. Oki, *Applications of Dynamic NMR Spectroscopy to Organic Chemistry* (VCH, Florida, 1985); U. Berg, T. Liljefors, C. Roussel, and J. Sandstrom, Acc. Chem. Res. **80**, 18 (1985).

[2] For a preliminary report of some of these results, see: P. J. Breen, J. A. Warren, E. R. Bernstein, and J. I. Seeman, J. Am. Chem. Soc. (submitted).

[3] J. I. Seeman, Chem. Rev. **83**, 83 (1983).

[4] T. M. Dunn, R. Tembreull, and D. M. Lubman, Chem. Phys. Lett. **121**, 453 (1985).

[5] A. Oikawa, H. Abe, N. Mikami, and M. Ito, J. Chem. Phys. **88**, 5180 (1984).

[6] K. Okuyama, N. Mikami, and M. Ito, J. Phys. Chem. **89**, 5617 (1985).

[7] P. J. Breen, J. A. Warren, E. R. Bernstein, and J. I. Seeman, J. Chem. Phys. **87**, 1927 (1987).

[8] E. R. Bernstein, K. Law, and M. Schauer, J. Chem. Phys. **80**, 207 (1984).

[9] (a) P. Groner and J. R. Durig, J. Chem. Phys. **66**, 1856 (1977); (b) P. Groner, J. F. Sullivan, and J. R. Durig, *Vibrational Spectra and Structure*, edited by J. R. Durig (Elsevier, New York, 1981), Vol. 9, p. 405.

[10] P. Bunker, *Molecular Symmetry and Spectroscopy* (Academic, London, 1979).

[11] H. C. Longuet-Higgins, Mol. Phys. **6**, 445 (1963).

[12] J. Kao, D. Leister, and M. Sito, Tetrahedron Lett. **26**, 2403 (1985); J. Kao, J. Am. Chem. Soc. (in press).

[13] J. I. Seeman, Pure Appl. Chem. (in press).

[14] J. Murakami, M. Ito, and K. Kaya, Chem. Phys. Lett. **80**, 203 (1981).

[15] H. D. Rudolph, H. Driezler, A. Jaeschke, and P. Wendling, Z. Naturforsch. Teil A **22**, 940 (1967).

[16] C. A. Wulff, J. Chem. Phys. **39**, 1227 (1963).

[17] J. I. Seeman, J. C. Schug, and J. W. Viers, J. Org. Chem. **48**, 2399 (1983).

[18] For related studies, see: J. Siegel, A. Gutierrez, W. B. Schweizer, O. Ermer, and K. Mislow, J. Am. Chem. Soc. **108**, 1569 (1986).

[19] K. M. Gough, B. R. Henry, and T. A. Wildman, J. Mol. Struct. **124**, 71 (1985).

[20] J. D. Cox and G. Pilcher, *Thermochemistry of Organic and Organometallic Compounds* (Academic, New York, 1970).

[21] W. R. Woolfenden and D. M. Grant, J. Am. Chem. Soc. **88**, 1496 (1966).

[22] E. E. Burnell and P. Diehl, Mol. Phys. **24**, 489 (1972).

[23] H. D. Rudolph, K. Walzer, and I. Krutzik, J. Mol. Spectrosc. **47**, 314 (1973).

[24] P. M. Stier, C. F. Barnett, and G. E. Evans, Phys. Rev. **96**, 973 (1954).

[25] R. C. Amme, J. Chem. Phys. **50**, 1891 (1969).

[26] K. C. Ingham and S. J. Strickler, J. Chem. Phys. **53**, 4313 (1970).

[27] Coupled rotation of two substituents is typically not observed in S_0. See Ref. 17.